



## **Fabrication and Characterization of PMMA/HMX-based Microcapsules *via in situ* Polymerization**

**Xinlei Jia, Conghua Hou, Yingxin Ton,\* Jingyu Wang, Baoyun Ye**

*School of Chemical Engineering and Environment,  
North University of China, Taiyuan, 030051, Shanxi, P. R. China  
\*E-mail: 1004024260@qq.com*

**Abstract:** Microcapsule technology was applied with nitramine explosives to improve their performance. Polymethyl Methacrylate (PMMA) was selected for the fabrication of 1,3,5,7-tetranitro-1,3,5,7-tetrazocane (HMX) based microcapsules. The PMMA/HMX-based microcapsules were prepared *via a facile in situ* polymerization of PMMA on the surface of the HMX crystals. Structural characterization of the PMMA/HMX microcapsules was studied systematically by scanning electron microscopy (SEM), X-ray diffraction (XRD), Fourier-transform infrared (FT-IR) spectroscopy, and their thermal durability as well as their mechanical sensitivities were measured. The results indicated that spherical microcapsules were formed, with PMMA as the capsule wall and HMX as the core material. The SEM results showed that the grains of the PMMA/HMX microcapsules were spherical and that the particle distribution was homogeneous. XRD and FT-IR analyses indicated that the HMX polymorph was preserved in the optimal  $\beta$ -form during the whole preparative process. The DSC results showed that the PMMA/HMX microcapsules had better thermal decomposition performance, and that the apparent activation energy of the microcapsules had increased by 47.3 kJ/mol compared to the recrystallized HMX, and its thermal stability had greatly improved. In addition, the drop height ( $H_{50}$ ) had increased from 30.45 cm to 58.49 cm, an increase of 65.81%. Thus, microcapsule technology will have a very wide range of applications in reducing the sensitivity of high energy materials in the future.

**Keywords:** fabrication, characterization, HMX, PMMA, microcapsules

## 1 Introduction

Micro-encapsulation is a new technology in which solid, liquid, or gas particles are surrounded by a layer of natural or synthetic polymer to give micron-size capsules [1]. It is used mainly to protect unstable or susceptible functional materials [2], isolate a core from its surroundings [3], retard leaching or volatilization of a volatile core [4], and improve the handling properties of sticky materials [5]. It has also recently found different applications in the pharmaceutical [6], food [7], paper [8], and textile industries [9].

Until now, micro-encapsulation has aroused increasing interest and has been frequently used whenever the functionality of an active substance needs to be protected or a controlled release is required [10, 11]. Researchers from different study groups have adopted recrystallization or coating technologies to desensitize existing explosives [12-15], and several strategies have been developed for the creation of polymer coated core-shell microcapsules, but the most commonly applied and industrially relevant method is *in situ* polymerization [16, 17]. With RDX as the core material, a water soluble protein for cyst wall microcapsules were prepared through single coacervation by Lee Jiangcun *et al.* [18] in 2007. Although the prepared microcapsules had good rheological behaviour and a high encapsulation rate, the morphology of the microencapsulated crystals was irregular. Cheng Zhengwei *et al.* discussed methods for the preparation of hydrophobic core materials [19], which laid a theoretical foundation for the preparation of HMX/PMMA microcapsules. HMX was coated *via in situ* crystallization with polyurethane by Gui Yu Zeng *et al.* [20] in 2011. The crystal morphology of HMX was complete but had large defects. Composites of graphene oxide/poly(methyl methacrylate) (GO/PMMA) were prepared through blending with simple solutions by Jing Dai *et al.* [21], the results providing a reference for the preparation of HMX/PMMA microcapsules. Hongguang Li *et al.* prepared TiO<sub>2</sub> precursor microcapsules *via* the interfacial crosslinking method [22], and explored the formation mechanism of the microcapsules. Microcapsules have been more widely adopted in some aspects of medicine, but are still relatively scarce in the energetic materials field.

Microencapsulation, starting from the internal composition and crystal structure of an explosive, is able to increase the oxygen balance, the critical heat and safety of the partial explosive, which can be used in the preparation of insensitive high-energy ammunition. Based on the theory of microcapsule preparation, spherical HMX/PMMA microcapsules were prepared by *in situ* polymerization. Their properties were characterized and provided a reference for the application of microcapsule technology in energetic materials.

## 2 Materials and Methods

### 2.1 Materials

HMX was provided by Gansu Yinguang Chemical Industry Group Co. Ltd. Methyl methacrylate (MMA) was obtained from Sinopharm Chemical Reagent Co. Ltd. Fluororubber (F<sub>2602</sub>) was provided by Sichuan Chenguang Chemical Co. Ltd. Azobisisobutyronitrile (AIBN) and polyvinyl alcohol (PVA) were purchased from Tianjin Guangfu Fine Chemical Industry Research Institute. Tween-80 and ethanol were provided by Tianjin Shen Tai Chemical Reagent Co. Ltd. Span-80 was obtained from Tianjin Damao chemical reagent factory.

### 2.2 Experimental processes

PMMA/HMX-based microcapsules were prepared *via in situ* polymerization. The experimental apparatus is shown in Figure 1. The experimental procedures were as follows: (i) Preparation of the HMX emulsion. Recrystallized HMX (4 g) and purified water (150 mL) were added to a 4-necked flask; (ii) The required quantities of composite emulsifier (0.2 g, formula  $M_{(\text{Tween-80})} : M_{(\text{Span-80})} = 53:47$ ) and auxiliary emulsifier (0.1 g PVA) were added to the flask, and the mixed solution was stirred evenly for 40 min at 500 rad/min in a bath at 45 °C. A uniform W/O emulsion was thus obtained; (iii) The initiator (0.0086 g AIBN) dissolved in methyl methacrylate (0.268 mL MMA), was then dropped into the 4-necked flask at the rate of 0.2 mL/min by rubber dropper; (iv) The system was gradually heated to 75 °C and the stirring was adjusted to 350 rad/min. The reaction conditions were maintained for 6 h under a nitrogen atmosphere (because the polymerization reaction would be inhibited in the presence of oxygen at lower than 100 °C; the whole process needs nitrogen protection); (v) The reaction was terminated and stood for 10 h; (vi) After filtration, the products were dried for 7 h using a freeze dryer to give HMX/PMMA microcapsules.

HMX/F<sub>2602</sub> and HMX/PMMA particles were prepared by the water suspension coating method in order to compare them with the properties of the HMX/PMMA microcapsules. The formulations were  $M_{(\text{Recrystallized HMX})} : M_{(\text{F2602})} = 95:5$ ,  $M_{(\text{Recrystallized HMX})} : M_{(\text{PMMA})} = 95:5$ .

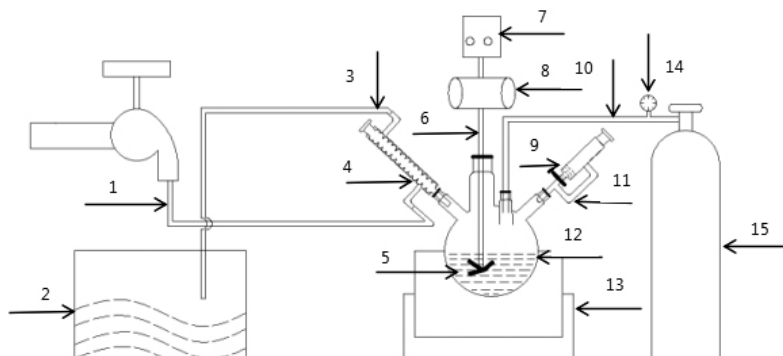


**Figure 1.** Experimental apparatus for the preparation microcapsules: 1. cooling water connection; 2. sink; 3. condenser outlet; 4. condenser; 5. emulsion 6. stirrer shaft; 7. S312 digital mixer; 8. motor; 9. prepolymer for microcapsule wall; 10. nitrogen protection; 11. constant-pressure funnel; 12. 4-necked flask; 13. digital intelligent thermostat oil bath; 14. control valve for reducing the nitrogen pressure; 15. nitrogen cylinder

### 2.3 Characterization

A field emission scanning electron microscope (FESEM, S4700 Hitachi, Ltd., Japan) was used to investigate the morphology, size and micro-structure of the capsules. The HMX/PMMA microcapsules obtained were dispersed on conductive carbon adhesive tape to attach to an FESEM stub, and then gold-coated. The crystal form of the HMX/PMMA microcapsules was determined by X-ray powder diffraction. The X-ray diffraction (XRD) patterns were recorded on a Bruker D8 Advance diffractometer with  $\text{Cu K}\alpha$  radiation. The infrared spectra were measured on a Nicolet 380 Fourier transform infrared (FTIR) spectrometer (KBr pellets, Thermo Fisher Scientific, Waltham, MA, USA). FTIR transmission spectra were generated using an FTIR spectrophotometer (Nicolet 6700, Thermo Scientific). The thermal properties were characterized by a Setaram DSC-131 (Setaram, Hillsborough Township, NJ, USA). The DSC conditions were as follows: sample mass: 0.7 mg; heating rate: 5 K/min, 10 K/min, 20 K/min; nitrogen atmosphere (flow rate : 20 mL/min). The impact sensitivity test conditions were: drop weight, 5 kg; sample mass, 35 mg. The impact sensitivity of each test sample was characterized by the drop height of 50% explosion probability ( $H_{50}$ ). Thus, a higher  $H_{50}$  value represents a reduced impact sensitivity.

### 3 Results and Discussion

#### 3.1 Reaction principle of PMMA micro-capsules

As shown in Figure 2, HMX is dispersed into emulsion droplets under mechanical agitation and emulsification; (ii) then, by dissolving AIBN in PMMA and adding the appropriate amount of water, the prepolymer is formed; (iii) through the action of a catalyst, the prepolymer undergoes addition polymerization, forming a water-soluble prepolymer; (iv) the prepolymer is gradually deposited on the surface of the HMX droplet and forms a capsule wall; (v) with the continuous deposition and polymerization of the prepolymer on the surface of the HMX, the density of the capsule wall increases and is coated to form a microcapsule.

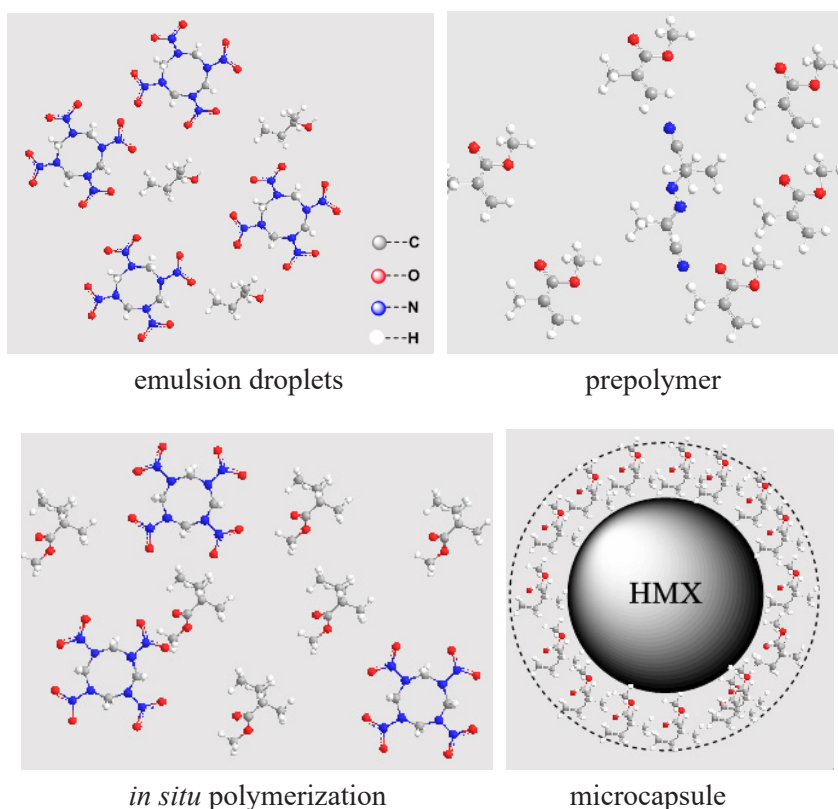


**Figure 2.** Proposed schematic mechanism for the core-shell coating *via in situ* polymerization

### 3.2 Morphological analysis

A field emission scanning electron microscope (FESEM, HITACHI S4700) was used to obtain typical SEM images of HMX (see Figure 3), and of the corresponding energetic microcapsules coated with PMMA. The raw HMX, which was purified by a careful recrystallization process, was uniform in size distribution with smooth crystal surfaces, and a particle size of about 1  $\mu\text{m}$ .

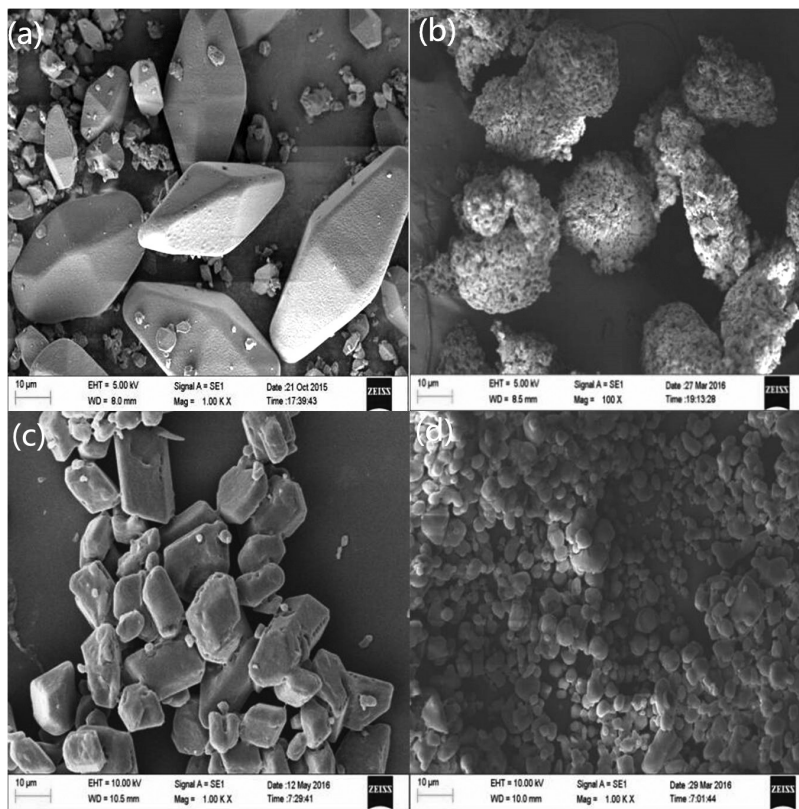


**Figure 3.** SEM images of recrystallized HMX (a), F<sub>2602</sub>/HMX (b), PMMA/HMX (c) and PMMA/HMX-based microcapsules (d)

Figure 3 displays typical SEM images of recrystallized HMX (3a), HMX coated with F<sub>2602</sub> and PMMA respectively, by the water suspension coating method (3b and 3c), and HMX microcapsules obtained *via in situ* polymerization of PMMA (3d). Obviously, the SEM image showed that recrystallized HMX had a polyhedral morphology and agglomeration. It may be clearly seen that the HMX based microcapsules exhibited obvious core-shell structures, which

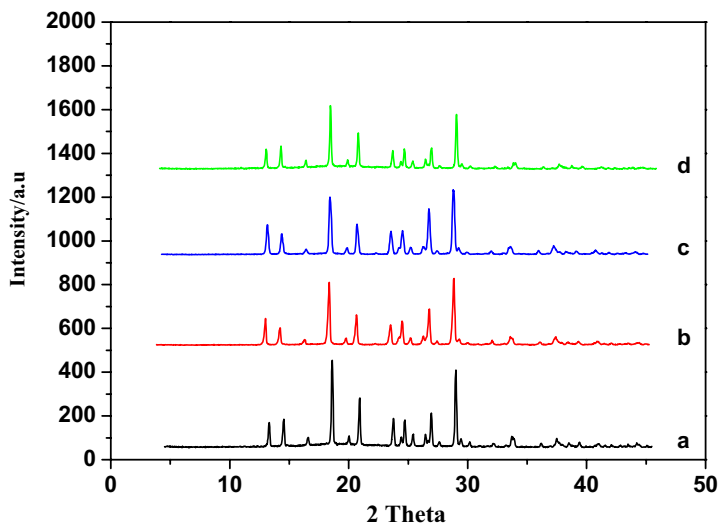
indicated that the microcapsules were successfully encapsulated by PMMA. Moreover, the PMMA formed compact and uniform coating shells around the whole surface of the HMX, and exhibited a high degree of coverage of HMX (Figure 3d). During the formation of the O/W emulsion, HMX particles interacted with each other by friction and collisions at high speed in the inert gas  $N_2$ . Then a homogeneously dispersed HMX emulsion was formed, assisted by a co-emulsifier (8% PVA can also work as a stable dispersing agent). Furthermore, assisted by the polymerization initiator, spherical microcapsules that consisted of core-HMX and shell-PMMA were formed.

### 3.3 XRD and FT-IR analyses

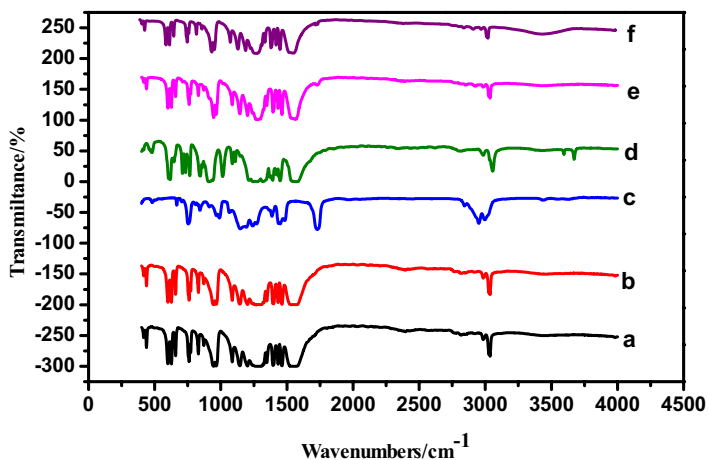
XRD and FT-IR analyses were conducted to investigate the crystal structure and component state of the energetic microcapsules prepared in this work. The results are presented in Figures 4 and 5, respectively.

Figure 4 shows the XRD patterns of recrystallized HMX,  $F_{2602}$ /HMX, PMMA/HMX and PMMA/HMX-based microcapsules. The HMX showed clear crystalline properties, with the characteristic diffraction peaks as determined in previous work. As may be seen from Figure 4, recrystallized HMX,  $F_{2602}$ /HMX, PMMA/HMX and PMMA/HMX-based microcapsules had similar diffraction peak angles, which indicates that the formation of  $F_{2602}$ /HMX, PMMA/HMX and PMMA/HMX-based microcapsules did not change the crystal form of HMX; its structure was still in the  $\beta$ -phase. It is interesting that the diffraction intensity of some peaks was slightly changed after recrystallized and coating (e.g. PMMA/HMX-based microcapsules: decreased intensity at  $2\theta$  of  $18.3^\circ$  and  $21.1^\circ$ ; PMMA/HMX: increased intensity at  $2\theta$  of  $26.8^\circ$ ). Such changes may be attributed to the decline of the quality of HMX after coating which is very common in crystallography.

In order to further study the crystals of the core-shell coating products, FTIR spectroscopy was used to characterize the samples, as may be seen in Figure 5. The characteristic peaks at  $1145\text{ cm}^{-1}$ ,  $2950\text{ cm}^{-1}$ , and  $1715\text{ cm}^{-1}$  were C–O–C,  $-\text{CH}_3$ ,  $-\text{C}=\text{O}$  in the infrared spectrum of PMMA; the characteristic vibration peaks at  $1569\text{ cm}^{-1}$  and  $2980\text{ cm}^{-1}$  were  $-\text{NO}_2$  and  $-\text{CH}_2$  in the infrared spectrum of HMX. From the characteristic bands of the microcapsules, we can see that there are stretching vibration peaks of C–O–C,  $-\text{NO}_2$ ,  $-\text{C}=\text{O}$ ,  $-\text{CH}_2$  and  $-\text{CH}_3$  at  $1200\text{ cm}^{-1}$ ,  $1565\text{ cm}^{-1}$ ,  $1720\text{ cm}^{-1}$ ,  $2984\text{ cm}^{-1}$  and  $3035\text{ cm}^{-1}$ . That is to say, the former includes all of the characteristic peaks of PMMA and HMX, the crystal structure in the microcapsules was still  $\beta$ -phase, which demonstrated that microcapsules were formed in the process of MMA polymerization. PMMA was coated successfully onto the HMX surface.



**Figure 4.** XRD patterns of (a) HMX, (b) F<sub>2602</sub>/HMX, (c) PMMA/HMX, (d) microcapsules



**Figure 5.** FTIR spectra of (a) F<sub>2602</sub>, (b) F<sub>2602</sub>/HMX, (c) PMMA, (d) HMX, (e) PMMA/HMX, (f) microcapsules

### 3.4 Thermodynamic analysis

Thermal stability is widely considered as a key characteristic for energetic materials [23]. The DSC analyses of recrystallized HMX, F<sub>2602</sub>/HMX, PMMA/HMX and PMMA/HMX-based microcapsule samples are shown in Figure 6.

In the DSC curves, the exothermic peak of recrystallized HMX, F<sub>2602</sub>/HMX,



PMMA/HMX and PMMA/HMX-based microcapsules increased as the heating rate was increased, the exothermic peak temperatures of recrystallized HMX being 280.18 °C, 284.08 °C, 289.37 °C at heating rates of 5 K/min, 10 K/min, 20 K/min, respectively. Similarly, the exothermic peak temperatures of the PMMA/HMX-based microcapsules were 281.11 °C, 284.9 °C, 289.15 °C at heating rates of 5 K/min, 10 K/min, 20 K/min, respectively, *i.e.* the temperature of the exothermic peak increased with increasing heating rate. In addition, the exothermic peak temperature of the PMMA/HMX-based microcapsules was higher than those of the other samples. Thus, the results indicated that the PMMA/HMX-based microcapsules had better thermal stability. Accordingly, from the three exothermic peaks of recrystallized HMX, the apparent activation energy, the frequency factor and the peak temperature when  $\beta_i$  is zero were determined by Kissinger's method [24, 25]. Furthermore, the thermal stability of the explosives can be calculated by Equations 2 and 3.

$$\ln\left(\frac{\beta_i}{T_{pi}^2}\right) = \ln\left(\frac{AR}{E_a}\right) - \frac{E_a}{RT_{pi}} \quad (1)$$

$$T_{pi} = T_{p0} + b\beta_i + c\beta_i^2 \quad (2)$$

$$T_b = \frac{E - \sqrt{E^2 - 4RET_{p0}}}{2R} \quad (3)$$

where  $E_a$  is the apparent activation energy;  $A$  is the frequency factor;  $T$  is the absolute temperature;  $\beta_i$  is the heating rate (in K/min);  $T_{p0}$  is the peak temperature when  $\beta_i$  is zero (in K);  $b$  and  $c$  are constants; and  $T_b$  is the critical explosion temperature (in K).

The test results were linearly fitted according to  $1/T$  as the ordinate and  $\ln(b/Tp^2)$  as the abscissa, as seen in Figure 7. As shown in Figure 7, a straight line was obtained when the values of  $\ln(b/Tp^2)$  were plotted against  $1/Tp$ , the activation energy may be calculated from the slope ( $-E/R$ ), and the pre-exponential factor may be calculated from the intercept [ $\ln(AR/E)$ ]. The fitting degrees for recrystallized HMX, F<sub>2602</sub>/HMX, PMMA/HMX and PMMA/HMX-based microcapsules activation energy were all greater than 99%, showing that the measurement data were accurate and reliable.

As indicated in Table 1, compared to recrystallized HMX, the apparent activation energies for coated HMX and PMMA/HMX-based microcapsules were all increased. The frequency factors were also increased. An interesting observation was that the apparent activation energy of the PMMA/HMX-based microcapsules had the most significant increase. More specifically, compared to

recrystallized HMX, the apparent activation energy of the PMMA/HMX-based microcapsules had increased by 47.3 kJ/mol, but that of F<sub>2602</sub>/HMX and PMMA/HMX has increased by only 3.96 kJ/mol and 15.26 kJ/mol respectively, which means that microcapsules have better thermal stability than coated HMX. This may be explained by the fact that the co-crystal has a higher crystal density due to microencapsulation. It is well known that an enthalpy change depends on the particle size, and the diameter of the microcapsules was smaller than that of the coated HMX. The smaller the particle size is, the greater is the surface area, so the decrease in adsorption capacity between the particles causes their activation energy to increase. In addition, the melting temperature of PMMA is about 160 °C, and increasing temperature generates free radicals. The instability of PMMA radicals would reduce the stability of the transition state, thus increasing the activation energy.

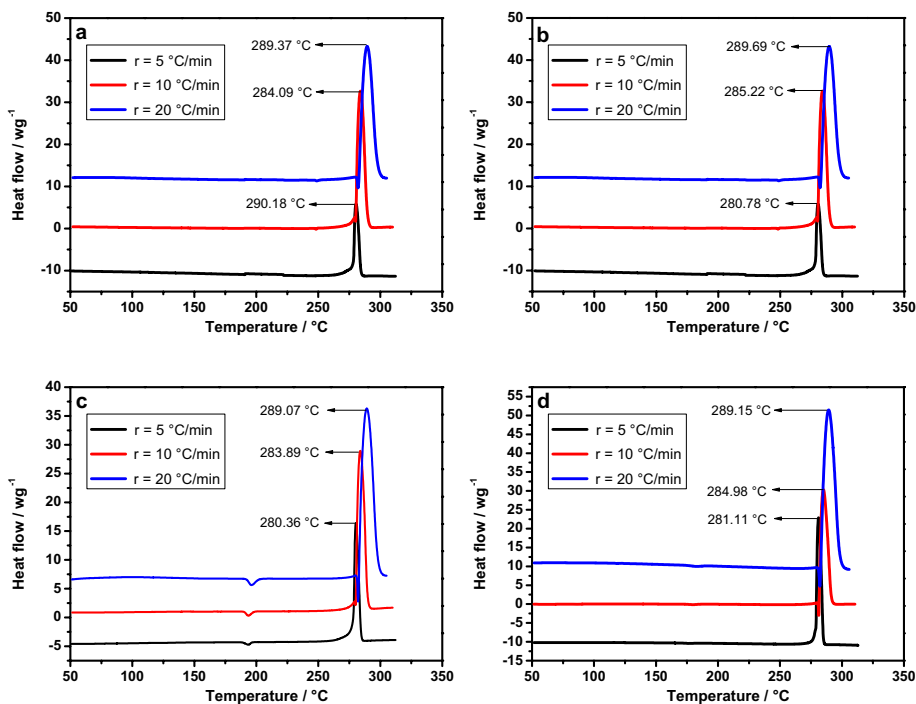


**Figure 6.** DSC curves of recrystallized HMX (a), F<sub>2602</sub>/HMX (b), PMMA/HMX (c) and PMMA/HMX-based microcapsules (d)

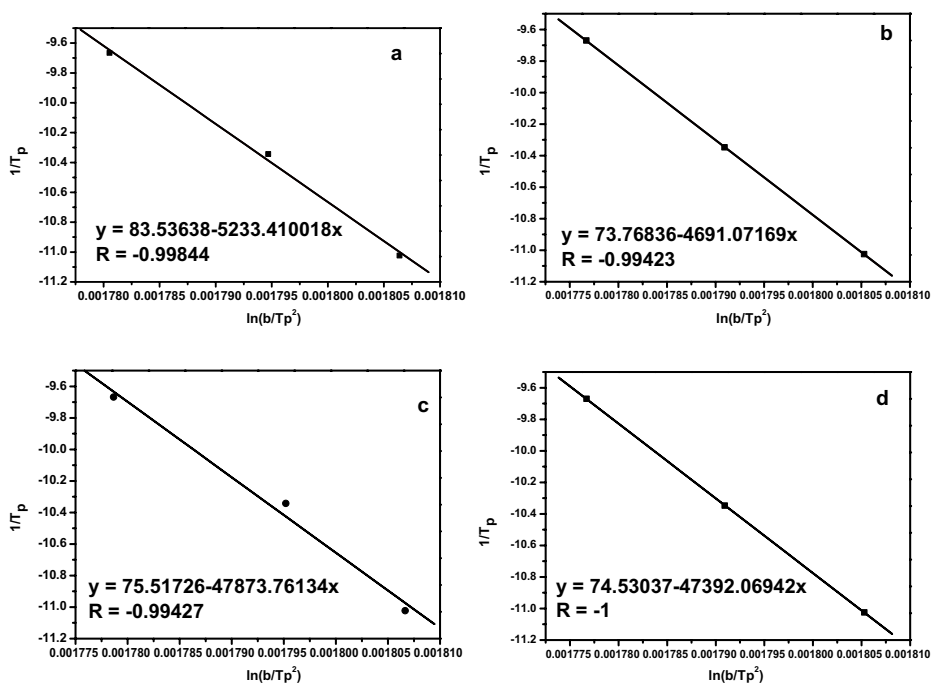


**Figure 7.** The linear fitted lines of recrystallized HMX (a),  $F_{2602}/\text{HMX}$  (b), PMMA/HMX (c) and PMMA/HMX-based microcapsules (d)

**Table 1.** Thermal decomposition kinetic parameters of different HMX samples

Samples	$E_a$ [kJ/mol]	$A$	$T_{p0}$ [°C]	$T_b$ [°C]
Recrystallized HMX	390.06	$4.11 \times 10^{35}$	276.24	277.89
$F_{2602}/\text{HMX}$	394.02	$1.11 \times 10^{37}$	274.9	276.5
PMMA/HMX	405.32	$3.00 \times 10^{37}$	276.20	276.2
Microcapsules	437.36	$1.43 \times 10^{41}$	276.05	277.51

### 3.5 Impact sensitivity

The impact sensitivities of recrystallized HMX,  $F_{2602}/\text{HMX}$ , PMMA/HMX and PMMA/HMX-based microcapsules were tested. The results are presented in Table 2.

It may be seen from Table 2 that compared to recrystallized HMX, the drop height for coated HMX has significantly improved. More specifically,  $H_{50}$  of  $F_{2602}/\text{HMX}$  and PMMA/HMX were 1.54 times and 1.19 times respectively that of recrystallized HMX, but  $H_{50}$  of the microcapsules was 1.72 times that of recrystallized HMX, and the impact sensitivity has been further reduced. This

is because for the same quality of HMX, when the particle size is smaller, the spherical effect is stronger, and the surface area is larger [26]. The pressure on HMX with the ball falling from the same height became less, so the  $H_{50}$  of the microcapsules has been markedly enhanced compared to HMX that was simply coated.

**Table 2.** Impact sensitivity of recrystallized HMX,  $F_{2602}$ /HMX, PMMA/HMX and microcapsules

Samples	$H_{50}$ [cm]	Standard deviation
Recrystallized HMX	34.05	0.037
$F_{2602}$ /HMX	39.32	0.063
PMMA/HMX	40.47	0.061
Microcapsules	58.49	0.052

## 4 Conclusions

Spherical microcapsules were formed with PMMA as the capsule wall and HMX as the core material. The SEM results showed that the grains of the PMMA/HMX microcapsules were solid spherical and the particle distribution was homogeneous. XRD and FT-IR analyses showed that the polymorph of HMX was maintained in the optimal  $\beta$ -form during the whole preparative process. The apparent activation energy (thermal decomposition) of the microcapsules had increased by 47.3 kJ/mol compared to that of recrystallized HMX, and the thermal stability of the microcapsules had greatly improved.  $H_{50}$  increased from 30.45 cm to 58.49 cm, and the impact sensitivity had decreased by 65.81%. In the future, microcapsule technology will have a very wide range of applications in reducing the sensitivity of high energy materials.

## References

- [1] Kondo, A. *Microcapsule Processing and Technology*. Marcel Dekker, **1979**; ISBN 9780824768577.
- [2] *Microencapsulation: Methods and Industrial Applications*. CRC Press, **2005**; ISBN 9780824723170.
- [3] Lu, R.; Dou, H.; Qiu, Y.; Zhang, D; Sun, K.. Polymeric Microcapsules with Internal Cavities for Ultrasonic Imaging: Efficient Fabrication and Physical Characterization. *Colloid Polym. Sci.* **2009**, 287(6): 683-693.

- [4] Griss, P.; Andersson, H.; Stemme, G. Expandable Microspheres for the Handling of Liquids. *Lab Chip* **2002**, *2*(2): 117-120.
- [5] Kim, Y. D.; Morr, C. V. Microencapsulation Properties of Gum Arabic and Several Food Proteins: Spray-Dried Orange Oil Emulsion Particles. *J. Agric. Food Chem.* **1996**, *44*(5): 1314-1320.
- [6] Cook, M. T.; Tzortzis, G.; Charalampopoulos, D.; Khutoryanskiy, V. V. Microencapsulation of Probiotics for Gastrointestinal Delivery. *J. Controlled Release* **2012**, *162*(1): 56-67.
- [7] Nazzaro, F.; Orlando, P.; Fratianni, F.; Coppola, R. Microencapsulation in Food Science and Biotechnology. *Curr. Opin. Biotechnol.* **2012**, *23*(2): 182-186.
- [8] Aziz, F. R. A.; Jai, J.; Raslan, R.; Subuki, I. Microencapsulation of Essential Oils Application in Textile: A Review. *Adv. Mater. Res. (Durnten-Zurich, Switz.)* **2015**, 1113.
- [9] Vandegaer, J. E. *Microencapsulation: Processes and Applications*. Springer Science & Business Media, **2012**; ISBN 9781468407419.
- [10] NeoDauer, M. P.; Poehlmann, M.; Fery, A. Microcapsule Mechanics : from Stability to Function. *Adv. Colloid interface* **2014**, *207*: 65-80.
- [11] Pretazl, M.; Neubauer, M.; Tekaat, M.; Kunert, C.; Kuttner, C.; Leon, G.; Berthier, D.; Erni, P.; Quali, L.; Fery, A. Formation and Mechanical Characterization of Aminoplast Core-Shell Microcapsules. *ACS Appl. Mater. Interfaces* **2012**, (4): 2940-2948.
- [12] Kröber, H.; Teipel, U. Crystallization of Insensitive HMX. *Propellants Explos. Pyrotech.* **2008**, *33*(1): 33-36.
- [13] Van der Heijden, A. E. D. M.; Creyghton, Y. L. M.; Marino, E.; Bouma, B.; Duvalois, W. Energetic Materials: Crystallization, Characterization and Insensitive Plastic Bonded Explosives. *Propellants Explos. Pyrotech.* **2008**, *33*(1): 25-32.
- [14] Song, X.; Wang, Y.; An, C.; Guo, X.; Li, F. Dependence of Particle Morphology and Size on the Mechanical Sensitivity and Thermal Stability of Octahydro-1,3,5,7-tetranitro-1,3,5,7-tetrazocine. *J. Hazard. Mater.* **2008**, *159*(2): 222-229.
- [15] Ji, W.; Li, X.; Wang, J.; Ye, B.; Wang, C. Preparation and Characterization of the Solid Spherical HMX/F<sub>2602</sub> by the Suspension Spray-Drying Method. *J. Energ. Mater.* **2016**, *34*(4): 357-367.
- [16] Su, J. F.; Schlangen, E. Synthesis and Physicochemical Properties of High Compact Microcapsules Containing Rejuvenator Applied in Asphalt. *Chem. Eng. J.* **2012**, *198*: 289-300.
- [17] Roghani-Mamaqani, H.; Haddadi-Asl, V.; Salami-Kalajahi, M. In Situ Controlled Radical Polymerization: a Review on Synthesis of Well-Defined Nanocomposites. *Polym. Rev.* **2012**, *52*: 142-188.
- [18] Li, J. C.; Jiao, Q. J.; Ren, H.; Wang, L. X.; Zhao, W. D. Study on Processing Parameters of RDX Micro-capsule Coated by Protein. *Initiators & Pyrotechnics (Huogongpin)* **2007**, 1-5.
- [19] Cheng, Z. W.; Bao, Z. H. Fabrication and Characterization of Solid-Core Material Microcapsulation. *Polym. Bull.* **2010**, 55-60.

- [20] Zeng, G. Y.; Nie, F. D.; Liu, L.; Chen, J.; Huang, H. In Situ Crystallization Coating HMX by Polyurethane. *Chin. J. Energ. Mater. (Hanneng Cailiao)* **2011**, 138-141.
- [21] Dai, Jing.; Lang, M. Preparation and Mechanical Properties of Graphene Oxide/PMMA and Surface-Functionalized Graphene/PMMA Composites. *Acta Chim. Sin. (Engl. Ed.)* **2012**, 1237-1244.
- [22] Li, H. G.; Yan, J.; Wang, M. Q.; Meng, S. H.; Du, S. G. Microcapsulation of TiO<sub>2</sub> Precursor and Its Performance as Inhibitor of Erosion. *J. Inorg. Mater.* **2015**, 47-52.
- [23] Yan, Q. L.; Zeman, S. Theoretical Evaluation of Sensitivity and Thermal Stability for High Explosives Based on Quantum Chemistry Methods: a Brief Review. *Int. J. Quantum Chem.* **2013**, 113: 1049-1061.
- [24] Kissinger, H. E. Reaction Kinetics in Differential Thermal Analysis. *Anal. Chem.* **1957**, 29(11): 1702-1706.
- [25] Sha, W. Determination of Activation Energy of Phase Transformation and Recrystallization Using a Modified Kissinger Method. *Metall. Mater. Trans. A* **2001**, 32: 2903-2904.
- [26] Doherty, M.; Watt, D. S. Relationship between RDX Properties and Sensitivity. *Propellants Explos. Pyrotech.* **2008**, 33: 4-13.